Structure of β_2-bungarotoxin: potassium channel binding by Kunitz modules and targeted phospholipase action

Peter D Kwong[1], Neil Q McDonald[1†], Paul B Sigler[3] and Wayne A Hendrickson[1,2*]

[1]Department of Biochemistry and Molecular Biophysics and [2]Howard Hughes Medical Institute, Columbia University, New York, NY 10032, USA and [3]Department of Molecular Biophysics and Biochemistry and Howard Hughes Medical Institute, Yale University, New Haven, CT 06511, USA

Background: β-bungarotoxin is a heterodimeric neurotoxin consisting of a phospholipase subunit linked by a disulfide bond to a K^+ channel binding subunit which is a member of the Kunitz protease inhibitor superfamily. Toxicity, characterized by blockage of neural transmission, is achieved by the lipolytic action of the phospholipase targeted to the presynaptic membrane by the Kunitz module.

Results: The crystal structure at 2.45 Å resolution suggests that the ion channel binding region of the Kunitz subunit is at the opposite end of the module from the loop typically involved in protease binding. Analysis of the phospholipase subunit reveals a partially occluded substrate-binding surface and reduced hydrophobicity.

Conclusions: Molecular recognition by this Kunitz module appears to diverge considerably from more conventional superfamily members. The ion channel binding region identified here may mimic the regulatory interaction of endogenous neuropeptides. Adaptations of the phospholipase subunit make it uniquely suited to targeting and explain the remarkable ability of the toxin to avoid binding to non-target membranes. Insight into the mechanism of β-bungarotoxin gained here may lead to the development of therapeutic strategies against not only pathological cells, but also enveloped viruses.

Structure 15 October 1995, **3**:1109–1119

Key words: Kunitz module, molecular recognition, neurotoxin, phospholipase, potassium channel, targeted toxin

Introduction

The venoms of many poisonous animals contain a diverse cocktail of toxins, often neurotoxins, conferring potency against a spectrum of targets and prey (reviewed in [1,2]). For example, venom from the snake *Bungarus multicinctus* contains both α-bungarotoxin, which blocks acetylcholine receptors on the postsynaptic membrane of neuromuscular junctions, and β-bungarotoxin, a completely unrelated protein, which inhibits neurotransmitter release from presynaptic membranes [3,4]. Diversity in targets of action is supplemented by further heterogeneity in each toxic component. A κ-homolog of α-bungarotoxin has specificity for neuronal over neuromuscular receptors [5], and there are many isoforms of β-bungarotoxins. These β-bungarotoxin isoforms are heterodimeric proteins, and diversity arises from combinatorial associations of variants of each subunit. Six different β-bungarotoxin isoforms (designated β_1–β_6) have been identified by sequencing, and their differential activities have been partially characterized [6,7].

Each β-bungarotoxin dimer has a phospholipase A_2 subunit covalently coupled through a disulfide link to a smaller subunit related to Kunitz-type protease inhibitors [6]. Both components are members of well-studied protein families, with more than a dozen atomic-level structures known for representatives of each. Sequences of the enzymatic subunit closely resemble those of other extracellular A_2-specific phospholipases which are found in pancreatic secretions, inflammatory exudates and certain toxins ([8], reviewed in [9]). It is the lipolytic action of β-bungarotoxin, directly responsible for the depolarizing permeabilization of the synaptosomal plasma membrane, that characterizes its toxicity [10]. Sequences of the smaller subunit identify them as members of the Kunitz (Kunin or pancreatic trypsin type) protease inhibitor superfamily ([6], reviewed in [11,12]), although β-bungarotoxin has no protease inhibitor capacity [6]. Instead, the β-bungarotoxin Kunitz subunit serves to guide the toxin to its site of action on the presynaptic membrane by virtue of a high-affinity interaction (nanomolar K_d) with a specific subclass of voltage-sensitive potassium channels [13–15]. Although the phospholipase/Kunitz combination is unique to β-bungarotoxin, other toxins are known to be based separately on either phospholipase or Kunitz-type proteins.

A number of venom phospholipases are toxic (reviewed in [16]) and, although they appear to share similar biochemical properties [17], they vary mechanistically. For example, the neurotoxin crotoxin is composed of a standard phospholipase and an inhibitory chaperone, which blocks the phospholipase active site until binding to a presynaptic receptor triggers the dissociation of the chaperone [18]. In contrast, both the monomeric phospholipase from *Oxyuranus scutellatus* and notexin from *Notechis scutatus scutatus* are unchaperoned; the former has a specific skeletal muscle receptor [19],

*Corresponding author. †Present address: ICRF Unit for Structural Biology, Birkbeck College, Malet Street, London, WC1E 7HX, UK.

 ISSN 0969-2126

whereas notexin targets the neuromuscular junction [20]. Among all known phospholipase toxins, only β-bungarotoxin has a mechanism of action in which targeting and phospholipase activity are separated into non-homologous subunits.

Other Kunitz toxins of known structure include α-dendrotoxin and its relatives, toxin I and toxin K [21–23]. The mode of action of these toxins is both similar and different from that of β-bungarotoxin. They also bind tightly to certain voltage-gated potassium channels on presynaptic membranes, but their mode of action is channel blockage, which in turn facilitates neurotransmitter release and leads to convulsions. Although their effects are opposite, and ultimately toxic, binding by β-bungarotoxin and α-dendrotoxin is similar. Thus, β-bungarotoxin binding can be inhibited by dendrotoxin [24] and the Kunitz subunit from β-bungarotoxin (prepared by reduction and carboxymethylation) binds with high affinity and blocks both non-inactivating and inactivating voltage-gated channels [25]. Indeed, in the early stage of β-bungarotoxin action, miniature end-plate potentials are actually increased and only later, presumably associated with phospholipase action, are they abolished [26]. Because of its primary role in guiding the toxin, we have termed the Kunitz subunit the 'targeting subunit' and we refer to the mechanism by which β-bungarotoxin acts as 'targeted phospholipase' action.

There is interest in therapeutic applications of toxins, and Kunitz toxins have been the focus of drug design efforts ([27], reviewed in [28]). By analogy with immunotoxins (reviewed in [29,30]), the bipartite structure of β-bungarotoxin may make it useful in the design of appropriately directed toxins. β-bungarotoxin has potential advantages in this respect. Unlike other highly toxic phospholipases, it is extremely specific in its effects and has neither direct nor indirect hemolytic activity [31]. Moreover, at concentrations of only 1–2 nM, it specifically suppresses the *in vitro* growth of neuronal cells while maintaining a high population of viable photoreceptor cells [32].

We report here the crystal structure of the β_2-isoform of β-bungarotoxin. Despite expected similarity in overall structure between the individual β-bungarotoxin subunits and their respective homologs, each has distinctive features. Comparative analyses, made in light of these features and the mode of intersubunit association defined by the structure, reveal surprisingly novel modes of interaction between this toxin and ion channels and lipid membranes. Insight into these interactions may be useful in other contexts: we discuss the relevance of toxin binding to ion-channel regulation and the therapeutic potential of a redirected phospholipase against enveloped viruses such as HIV.

Results

Overall structure

The structure of β_2-bungarotoxin was solved at 2.45 Å resolution by a combination of molecular replacement and multiple isomorphous replacement (MIR) phasing techniques and refined to an R value of 19.3%. The structure of β_2-bungarotoxin is shown schematically in Figure 1a. Although each subunit is essentially globular, their joining produces a relatively extended molecule of main-chain dimensions ~60 Å × 40 Å × 20 Å.

As expected from sequence analysis [7], the structure of the phospholipase subunit (120 residues and 6 disulfide bonds) closely resembles other members of a large family of homologous phospholipases A_2 [9]. Most of the backbone, including the three helices that constitute its core as well as the calcium-binding loop, superimpose well with the non-toxic class I phospholipase from *Naja naja atra* [8] (root mean square deviation [rmsd] of 0.826 Å for

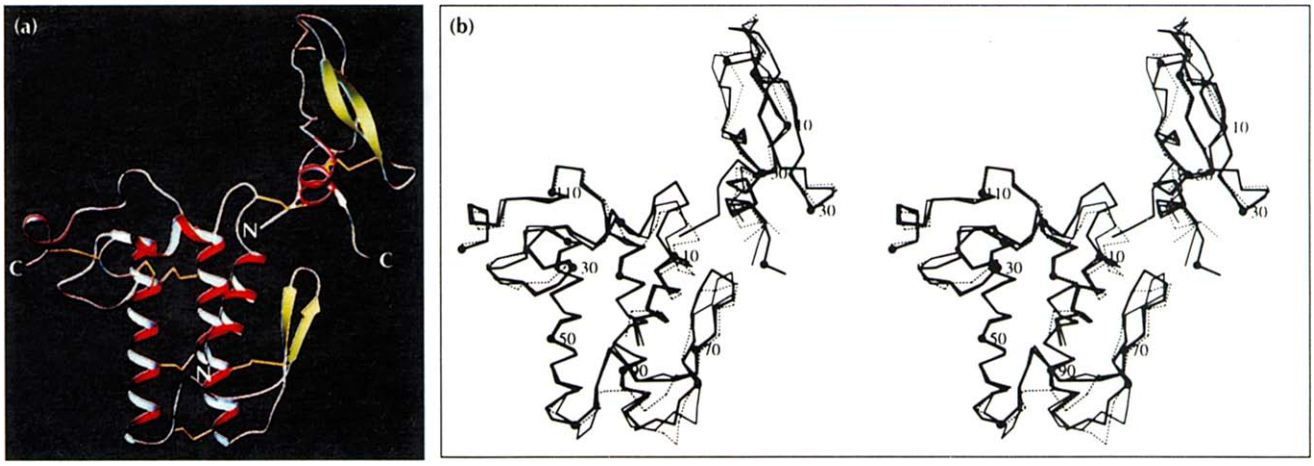

Fig. 1. Backbone structure of β_2-bungarotoxin. **(a)** Schematic displaying secondary structural elements. The smaller Kunitz subunit is shown at the top right connected through a disulfide bond to the larger phopholipase subunit. (Drawn with SETOR [75].) **(b)** Stereo plot of the Cα backbone of β_2-bungarotoxin shown superimposed with toxic (notexin and α-dendrotoxin; dashed line), and non-toxic (*Naja naja atra* phospholipase and BPTI; thin line) homologs of each subunit. Superpositions were made using all Cαs that remained within 2.5 Å of each other after least-squares alignment. Outliers are detailed in Figure 3. Spheres are drawn every 10 residues for reference. (Drawn with MOLSCRIPT [76].)

107 Cα atoms), and the toxic phospholipase notexin [33] (rmsd of 0.908 Å for 108 Cα atoms) (Fig. 1b). Differences are seen mainly in the regions that interact with the Kunitz subunit (residues 13–16 and 74–76), those close to the substrate-binding loop (residues 63–65), and those at the base of the so-called 'β wing' (residues 81–84).

The Kunitz subunit, with 61 residues and 3 disulfide bonds, also closely resembles other Kunitz superfamily members; it superimposes well with the classical protease inhibitor, bovine pancreatic trypsin inhibitor (BPTI) [34,35] (rmsd of 0.955 Å for 48 Cα atoms) and with the Kunitz toxin, α-dendrotoxin [21] (rmsd of 0.837 Å for 49 Cα atoms) (Fig. 1b). Differences are concentrated at the N terminus (which in β_2-bungarotoxin interacts with the phospholipase subunit) and in the region homologous to the anti-protease loop (which in conventional Kunitz protease inhibitors is involved in protease binding).

Anti-protease loop divergence

It was clear from the initial electron density that the region homologous to the anti-protease loop showed extensive structural rearrangements, when compared with BPTI (Fig. 2) [35]. The α-carbon of Gln17 in β_2-bungarotoxin is shifted 4.3 Å with respect to the homologous position of the active-site lysine of BPTI, and the neighboring disulfide adopts a substantially different orientation. The main-chain conformation here is stabilized by the buried side chain of Asp12, the carboxyl oxygen atoms of which hydrogen bond to the backbone nitrogen atoms of residues 14 and 42, both of which diverge considerably from the canonical Kunitz structure. Although a six amino acid insertion in the sequence of the acrosin inhibitor from *Drosophila funebris* [36] and the structure of a Tyr35→Gly mutant of BPTI [37] suggest that the protease-binding region is structurally malleable, dramatic rearrangements in the anti-protease loop itself are unprecedented.

Phospholipase substrate-binding loop

The phospholipase substrate-binding loop (encompassing roughly residues 60–70) is one of the most variable features of an otherwise extremely conserved family of phospholipases A_2. This loop was first identified by comparison of sequence and substrate preference, and its ability to influence substrate binding was confirmed by substitution mutagenesis [38]. In the substrate-binding loop of β_2-bungarotoxin, the contact residues (62–65), which map to within 2 Å of the superimposed substrate (see Fig. 3), differ substantially from the toxic phospholipase notexin (rmsd in backbone atoms of 5.6 Å), but are similar in structure to the non-toxic phospholipase *Naja naja atra* (rmsd in backbone atoms of 0.9 Å; Fig. 1b). Although differences with *Naja naja atra* phospholipase are found in the preceding residues (58–61), these do not interact with substrate. Thus, in contrast to the unforeseen divergence of the Kunitz subunit, the phospholipase substrate-binding loop appears to be similar in structure to non-toxic phospholipases.

Subunit interface

A novel Kunitz interaction is observed in β_2-bungarotoxin involving the intersubunit disulfide bridge at the C-terminal α helix (Cys55 of the Kunitz subunit linked to Cys15 of the phospholipase subunit). A detailed view of this portion of the molecule is shown in Figure 4.

Virtually all of the residues that make up the interface are charged. Only two of the intersubunit electrostatic interactions are direct — a salt bridge between Glu16 (phospholipase subunit) and Lys48 (Kunitz subunit), and a hydrogen bond involving the side chain of Arg75 (phospholipase) and the carbonyl oxygen atom of Leu58 (Kunitz) (Fig. 4). Other electrostatic interactions are water-mediated. For example, the interaction between the backbone nitrogen atom of Cys15 (phospholipase) and the side-chain oxygen atom of Glu56 (Kunitz), and a three-way interaction between the carbonyl oxygen atom of Cys55 (Kunitz) and the side-chain nitrogen atoms of Arg75 (phospholipase) and Arg1 (Kunitz) (Fig. 4).

Although interface residues are mostly charged, substantial hydrophobic interactions are found, involving primarily Tyr60 (Kunitz) as well as the aliphatic portions of Lys74 (phospholipase), Arg75 (phospholipase) and Arg1 (Kunitz). The subunit interface buries 1052 $Å^2$, with 145 $Å^2$ contributed by the half-cystine residues. The largest contributor is Arg75 (phospholipase) with 173 $Å^2$

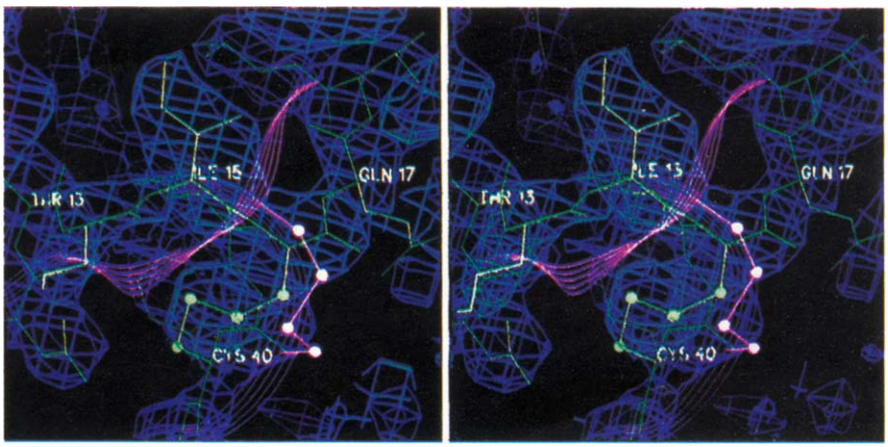

Fig. 2. Stereo diagram of electron density produced by combining the MIR and the phospholipase molecular replacement phases. Density distributions were calculated with data from 10–2.9 Å, and contoured at 1.0σ. The region shown is homologous to the anti-protease loop in the Kunitz subunit and cannot be biased by phase information from the phospholipase model. Shown with it are the final β_2-bungarotoxin refined model (light green) and a ribbon trace of the backbone and disulfides of BPTI (pink), superimposed as described in Figure 1. (Figure made with SETOR [75].)

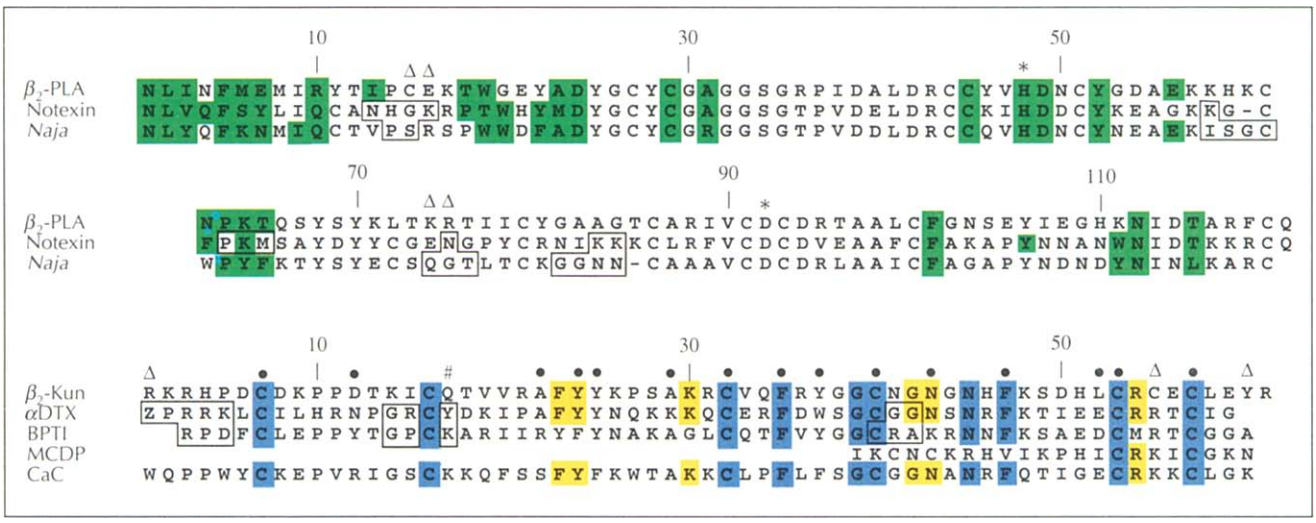

Fig. 3. Sequence of β_2-bungarotoxin aligned with subunit homologs. The sequence of β_2-bungarotoxin was redetermined. It is shown aligned with toxic and non-toxic homologs of each subunit: phospholipase subunit (notexin and *Naja naja atra* phospholipase) and Kunitz subunit (α-dendrotoxin [αDTX] and BPTI). These sequences have been aligned based on the superposition of their crystal structures (Fig. 1). Also shown for the Kunitz subunit are the sequences of two ion channel toxins, mast cell degranulating peptide (MCDP) and calcicludine (CaC), although less structural detail is available for them. Yellow, sequence conserved only among Kunitz toxins; blue, sequence conserved between all Kunitz toxins and BPTI; green, side chains within 2 Å of the surface as defined by the substrate acyl chains (see the Materials and methods section); *, catalytic residues in the phospholipase; #, reactive-site lysine or arginine residue of Kunitz serine protease inhibitors; Δ, intermolecular half-cystines and residues with >25% of their solvent-accessible surface buried in the subunit interface; ●, buried amino acid side chains of the Kunitz subunit of β_2-bungarotoxin with solvent accessibilities <15%; boxed, residues which differ from β_2-bungarotoxin by more than 2.5 Å after alignment as detailed in Figure 1.

buried, followed closely by Arg201 (Kunitz) with 167 Å^2. Charged or polar residues contribute the majority of the buried surface (987 Å^2). Except for the intersubunit cysteines, only five residues bury more than 25% of their surface area in the interaction (marked by Δ in Fig. 3).

The interface is long, but relatively narrow (dimensions of ~25 Å × 6 Å), possibly allowing for rotational mobility around the long axis of the interface. Contributing to this intersubunit mobility may be the flexibility of the interface contacts, most of which are side chain to side chain. No backbone to backbone contacts are found. In particular, the dominance of arginine and lysine residues, both of which can adopt many different conformations, may contribute to this mobility.

A β-bungarotoxin-like intermolecular disulfide bridge may also be present in the C-terminal domain of the morphogen Noggin, a dorsalization factor involved in head formation in *Xenopus* oocytes [39,40]. However, apart from the conserved cysteine, none of the residues identified as stabilizing the β_2-bungarotoxin interface are retained in Noggin.

Discussion

Structure analysis

With more than a dozen structures known at atomic resolution for representative members of each β-bungarotoxin subunit, the structure of β_2-bungarotoxin provides a unique opportunity for understanding the essential modifications needed for neurotoxicity, and more generally, for targeted toxicity. Several puzzles present themselves. First, although the structures of several toxin members of the Kunitz superfamily have been solved previously [21–23], the location of the ion channel binding region on the Kunitz module remains unknown. Second, the structure of the β-bungarotoxin phospholipase subunit superficially resembles non-toxic phospholipases. However, the toxin clearly differs from non-toxic phospholipases biochemically [17] and possesses the unexplained ability to avoid non-target membranes *en route* to the neurosynapse. In an attempt to decipher these puzzles, we combined structure analysis with biochemical data, sequence analysis, and mutagenesis results in an attempt to fully exploit the information gained from the structure solution.

Ion channel binding motif

The toxin members of the Kunitz superfamily bind to voltage-sensitive ion channels, primarily K^+ channels, although one member, calcicludine, is a potent blocker of voltage-sensitive Ca^{2+} channels [41]. Speculation concerning the interaction of Kunitz modules with ion channels has focused on whether it can be modeled following the protease–inhibitor paradigm of more conventional members of this superfamily. Results from toxin sequence analysis are unclear [42–44]. Nevertheless, it seems reasonable to suppose that because the Kunitz toxins all share the same fold, the structural features underlying their recognition of ion channels may be conserved.

We have compared the structures and sequences of four K^+ channel binding members of the Kunitz superfamily

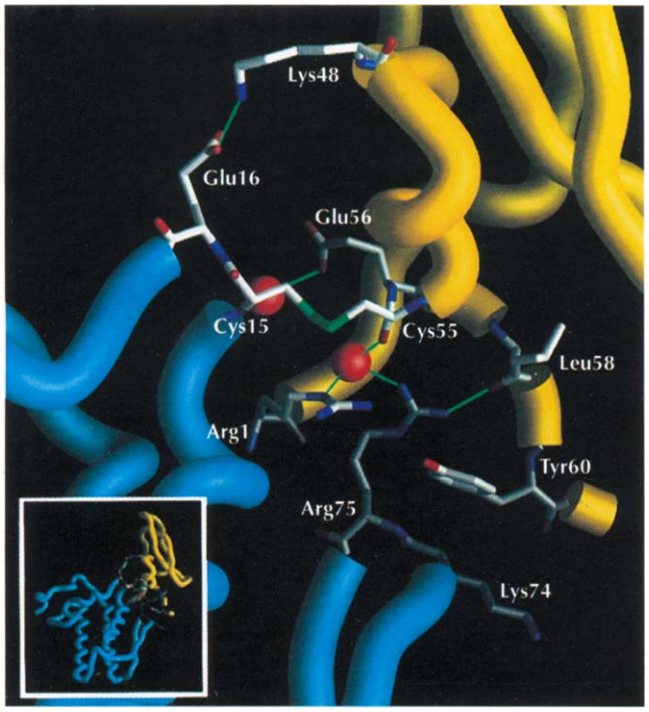

Fig. 4. β_2-bungarotoxin subunit interface. Interface residues depicted here have >25% of their surface buried in the interface or are involved in intersubunit hydrogen bonds. All other residues are represented by a backbone worm: Kunitz subunit (yellow), phospholipase subunit (cyan). Side chains of interface residues are colored by atom type: nitrogen (blue), oxygen (red), carbon (white) and sulfur (green). The two water molecules that mediate intersubunit hydrogen bonds are represented by red CPK spheres. Hydrogen bonds are shown as thin green lines. (Inset) For reference, a reduced picture of β_2-bungarotoxin in the same orientation. (Figure made with GRASP [56].)

(β_2-bungarotoxin, α-dendrotoxin [21], toxin I [22] and toxin K [23]). Residues likely to belong to the ion channel binding region were identified by the following criteria: solvent accessibility greater than 15%; conservation of amino acid identity within the Kunitz neurotoxins and not in BPTI; and preservation of main-chain orientation. When mapped on to the molecular surface of β_2-bungarotoxin, the results provide a striking identification of the general region likely to be involved in ion channel binding (Fig. 5a). Analogous criteria, when applied to the protease inhibitor members of the Kunitz superfamily, similarly identify the region of the anti-protease loop (Fig. 5b,c). The proposed ion channel binding region is located roughly 30 Å from the anti-protease loop at the opposite end of the module (Fig. 6). This region has not been previously implicated in molecular recognition events involving members of the Kunitz superfamily.

The identified region is an elongated basic surface which, judging by the relative orientation of the preserved interfacial binding surface of the phospholipase [8,9] (which contains the access route to the phospholipase active site), would face the membrane (Fig. 6). Residues specified by our criteria are Phe23 (tyrosine in BPTI) and Lys30 and Arg54 (glycine and methionine respectively in BPTI).

In all of the toxin structures for which side-chain conformations have been described, the orientations for Lys30 and Arg54 are similar. For Arg54, this conservation results in part from the support of its nominally flexible aliphatic Cβ and Cγ atoms by a conserved hydrophobic residue at position 58 (glycine in BPTI), one turn below it in the α helix. Sequence searches of the Swiss Protein data bank, and of previously published venom inhibitor homologs [41–43], demonstrate that the combination of Lys30, Arg54 and hydrophobic 58 is specific to toxins. Moreover, recent mutagenesis studies on toxin K confirm that part of the general region that we have identified here, the β turn (residues 27–30), is involved in ion channel binding (LA Smith, personal communication).

Relation of toxin binding to endogenous neuropeptides

Chimeric studies on dendrotoxin-sensitive and dendrotoxin-insensitive K^+ channels have defined a region of the ion channel that interacts with Kunitz toxins [45,46]. This region, the putative extracellular loop between the fifth and sixth transmembrane-spanning segments (S5 and S6), is thought to be important in regulating the extracellular channel mouth. It has been implicated in the binding of several K^+ channel toxins, including mast cell degranulating peptide (MCDP), which is a 22-amino acid peptide from bee venom [46,47]. Endogenous peptides that appear to be antigenically identical to MCDP, and which may induce long-term potentiation in the hippocampus, have been identified in porcine brain [48]. The structure of MCDP, as determined by NMR [49], contains a flexible tight turn and a CRXXC (where X is any residue) helix, that resemble, respectively, the Lys30 β turn and the Arg54-containing helix of β_2-bungarotoxin (Fig. 3). The structural similarity of MCDP to the proposed Kunitz ion channel binding motif combined with the interaction of MCDP (and presumably MCDP-like peptides) with the same portion of the ion channel suggests that, in contrast to other neuropeptides (which regulate K^+ channels indirectly through second messenger systems) these endogenous MCDP-like peptides may regulate their target K^+ channels through direct binding. The K^+ channel interaction of the Kunitz toxins may thus mimic the *in vivo* interaction of endogenous neuropeptides and serve as a biologically relevant model of direct K^+ channel regulation.

The prevailing paradigm of K^+ channel regulation holds that neuropeptides modulate K^+ channels indirectly, through second messenger systems. But neuropeptides have been found to function in a variety of ways ([50]; reviewed in [51,52]). The direct K^+ channel regulation by MCDP-like neuropeptides proposed here alters the prevailing paradigm, suggesting additional diversity of K^+ channel regulation. An analogous situation arises in the case of the Ca^{2+}-activated K^+ channel blocker apamin [53], for which the existence of endogenous apamin-like neuropeptides [54] indicates that direct K^+ channel regulation may operate here as well.

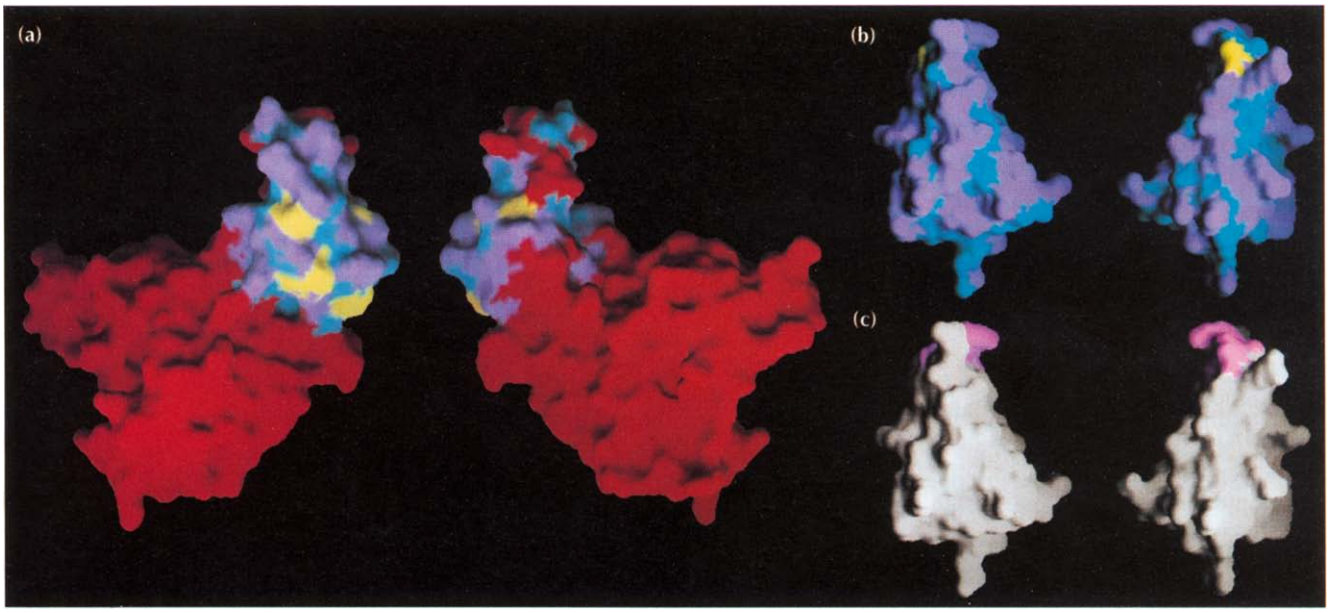

Fig. 5. Analysis of the molecular recognition surface of the Kunitz module. **(a)** β_2-bungarotoxin surface colored according to the sequence similarity of the underlying residues. The color scheme is similar to that of Figure 3: conserved only among Kunitz toxins (yellow), conserved between all Kunitz toxins and BPTI (blue), and non-conserved (purple). In addition, structurally diverse regions (where the backbone differed by >2.5 Å as detailed in Figure 3, and the phospholipase) are colored red. The yellow patch towards the center of the Kunitz subunit corresponds to Phe23. Clustered below it are Lys30 and Arg54. Two views of the toxin are shown related by a 180° rotation about a vertical axis. **(b)** Surface of BPTI colored with an analogous scheme (see the Materials and methods section for details). Residues are colored according to whether they are conserved only among protease inhibitors (yellow), conserved between protease inhibitors and β_2-bungarotoxin (blue), or not conserved (purple). The scale and orientation of BPTI here is analogous to that shown for the Kunitz subunit of β_2-bungarotoxin. Two views of BPTI are shown. **(c)** Protease inhibitor loop of BPTI: residues 12–16 (BPTI numbering) are shown in pink, all other residues in gray. (Figure made with GRASP [56].)

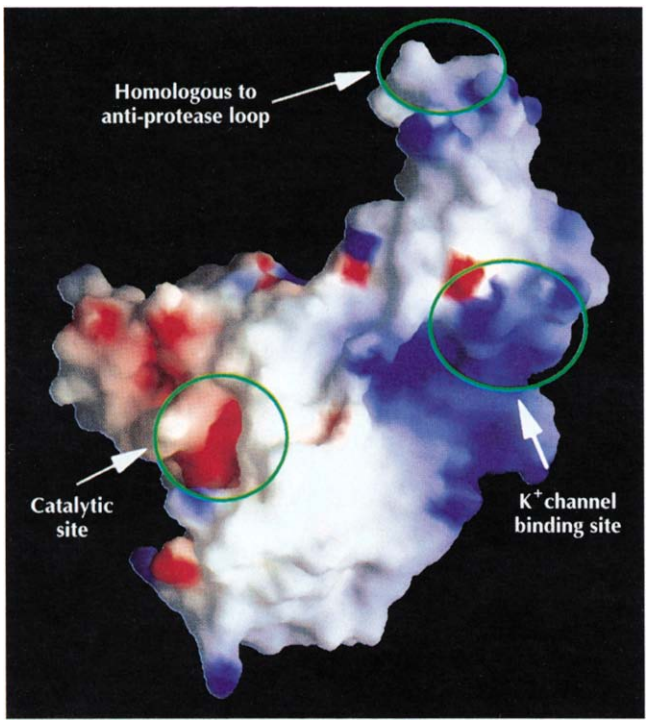

Fig. 6. Electrostatic potential at the molecular surface of β_2-bungarotoxin. Blue represents positive potential, red negative, and white neutral. The positions of selected features are highlighted. (Computed with GRASP [56] at neutral pH.)

Activity of the phospholipase subunit

The remarkable capacity of the toxin to avoid non-specific binding, and to hydrolyze the presynaptic membrane to the exclusion of others, is central to its neurotoxic action. Because the phospholipid substrate is continually present in abundance in non-target membranes, β-bungarotoxin faces special targeting problems. Even though the phospholipase subunit of the toxin has almost 60% sequence identity with other venom and pancreatic phospholipases, its interactions with membranes are biochemically different [17]. Non-toxic phospholipases bind membranes (and micelles) in a non-specific and promiscuous manner, whereas β-bungarotoxin binds poorly to zwitterionic and non-ionic micelles ($K_d \gg 60$ mM). In addition, it exhibits a much greater degree of selectivity for anionic surfaces than other phospholipases [17]. We analyzed the phospholipase subunit for clues to the functional adaptations required for targeted neurotoxicity.

Analysis of the structure of notexin [33], which when compared with other phospholipases displays a widely divergent substrate-binding loop, focused attention on this portion of the molecule. However, in β_2-bungarotoxin, the substrate-binding loop was found to be closely related to that of the non-toxic phospholipase from *Naja naja atra* (see Fig. 1b). Moreover, electrostatic analysis shows that the substrate-binding region of β_2-bungarotoxin is

negatively charged (Fig. 6), the same as its preferential binding surface (biochemically, it binds preferentially to anionic micelles [17]). While the overall charge of the toxin (+8 at neutral pH, most of which resides in the Kunitz subunit) may account for a non-specific affinity for anionic surfaces, other phospholipases have substantial net positive charges and are not neurotoxic (e.g. the eastern cottonmouth phospholipase has a net charge of +9 [55]). These observations tend to rule out conjectures explaining the toxic activity of β_2-bungarotoxin in terms of a structural binding feature or a specific electrostatic interaction.

We analyzed the chemical and physical properties of the β_2-bungarotoxin surface close to the substrate-binding site. The analysis takes advantage of the large number of high-resolution structures, several with bound substrate, which have been solved for this family of phospholipases. Surprisingly, β_2-bungarotoxin was found to segregate clearly from non-toxic phospholipases, showing both reduced hydrophobicity and reduced proximal surface area (Fig. 7). These two properties may be related through an association between surface curvature and hydrophobicity [56] and could account for the weak binding of the toxin to non-ionic micelles. They may also reflect a functional adaptation for neurotoxicity that reduces the non-specific affinity of the toxin for membranes and thereby enhances targeting specificity. Indeed, the other neurotoxic phospholipase included in the analysis, the monomeric notexin [33], segregates in the same fashion as β_2-bungarotoxin (Fig. 7a).

Crystal structures of several phospholipase A_2–substrate complexes demonstrate that this class of phospholipases binds substrate in a conserved manner [8]. Modeling of the phospholipid substrate into the active site of β_2-bungarotoxin leads to steric clashes with Trp19, which appears to partially occlude the hydrophobic substrate-binding site. Torsional rotation of Trp19 out of the active site — to the most favorable, sterically allowed, rotamer conformation [57] (and similar to that seen in the structure of the substrate complex of *Naja naja atra* phospholipase [8]) — would position its indole ring within the membrane. Such a conformation would increase both the hydrophobic and proximal surface area of the toxin by approximately 100 Å^2, aligning it with non-toxic phospholipases. Thus, while surface properties are a cumulative reflection of all of the exposed residues, Trp19 may play a central role by occluding the substrate-binding site during diffusion to the presynaptic membrane, and once at the membrane, acting as a hydrophobic anchor to facilitate tighter binding. Other phospholipases may also occlude their substrate-binding sites as a general mechanism for enhancing mobility; Trp19 is not unique to β_2-bungarotoxin and substrate-binding sites that are occluded by oligomeric interfaces have been observed in the crystal structures of several venom phospholipases [58,59].

Mechanism of β-bungarotoxin action

The structure of β_2-bungarotoxin illuminates some of the details of the β-bungarotoxin mechanism of action. In addition, the scenario presented here, although speculative, provides a convenient way to summarize the results of the structure analysis. After the toxin is injected by the snake, its partially occluded active site and reduced hydrophobicity enable it to avoid binding to non-target membranes and thus diffuse away from the site of injection. Upon reaching the presynaptic membrane, the Kunitz domain binds to its K^+ channel receptor through the binding region identified here. This initial K^+ channel binding is probably responsible for the observed transient increase in neurotransmitter release [25]. The K^+ channel is an integral membrane protein, and K^+ channel binding would presumably orient the phospholipase subunit towards the membrane (the K^+ channel binding region and the phospholipase active site are on the same face of the toxin; Fig. 6). The tight K^+ channel interaction would thus compensate for the decreased membrane affinity of the phospholipase. Once hydrolysis occurs, two events further enhance phospholipase affinity. First, substrate binding displaces Trp19, flipping it into the membrane where it provides a hydrophobic anchor. Second, fatty acids, released upon phospholipid hydrolysis, increase the anionic composition of the membrane, thereby enhancing β-bungarotoxin non-specific electrostatic affinity. Eventually, extensive phospholipid hydrolysis

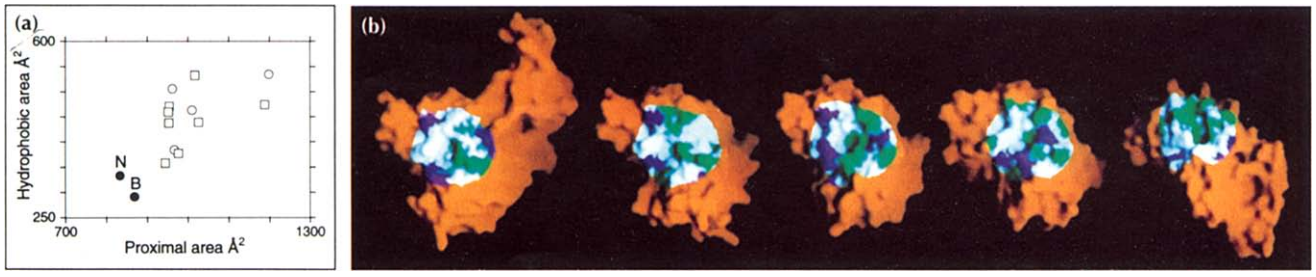

Fig. 7. Chemical and physical properties of the phospholipase surface proximal to the substrate-binding region. **(a)** Hydrophobic area and proximal area of the surface within 7.5 Å of the substrate acyl chains. Shown are (●) toxic phospholipases, (○) non-toxic phospholipases from structures without substrate, and (❑) non-toxic phospholipases from structures of substrate complexes. 'N' and 'B' label notexin and β_2-bungarotoxin respectively. **(b)** Phospholipase molecular surface colored by the physical properties of the underlying atoms: hydrophobic (green); charged (purple); polar (white). Portions of the surface that are >7.5 Å from the substrate acyl chains are colored orange. The surfaces depicted are (from left to right) β_2-bungarotoxin, notexin, and the phospholipases from cobra (*Naja naja atra* class I), rattlesnake (*Crotalus atrox* class II) and honeybee (*Apis mellifera* insect). (Figure made with GRASP [56].)

cumulatively interferes with neurotransmitter release, ultimately resulting in blockage of neural transmission, the hallmark of β-bungarotoxin neurotoxic action.

Therapeutic adaptation of β-bungarotoxin

The molecular mechanisms revealed here, by which β-bungarotoxin avoids non-specific membrane interactions, coupled with segregation of the targeting activity to a separate subunit (which may be removed by selective reduction; PDK unpublished data) make the β-bungarotoxin phospholipase uniquely suited to therapeutic adaptation. As with targeted toxin therapy, it should be possible to redirect the β-bungarotoxin phospholipase by switching its targeting subunit from the Kunitz module to, for example, a pathogen receptor or tumor-specific antibody. Such a redirected phospholipase would have several advantages over the typical targeted cytotoxins (such as ricin, exotoxin A, and cholera toxin) used in toxin therapy. In order to function, these other toxins must be internalized and translocated to the cytoplasm, which is a relatively inefficient process. Several thousand toxin molecules may be 'stranded' at the cell surface for each one that reaches the cytoplasm [28,60]. In contrast, the β-bungarotoxin phospholipase degrades membranes extracellularly. Such phospholipase therapy may also work on the virions of enveloped viruses (such as herpes, influenza, or retroviruses like HIV), which are resistant to conventional directed toxins. Indeed, because viruses lack cellular biosynthetic repair mechanisms they would be particularly susceptible to this type of membrane degradation.

Biological implications

The snake venom neurotoxin, β-bungarotoxin, is a heterodimer consisting of an enzymatic phospholipase subunit disulfide linked to a targeting subunit. The latter is a member of the toxin subfamily of the Kunitz protease inhibitor superfamily.

In the Kunitz subunit, residues 14–18, which are homologous to the anti-protease loop, adopt a markedly different conformation. Such divergence is unprecedented for the Kunitz superfamily and suggests that the previously observed conservation of this loop may reflect functional constraints rather than structural restrictions. This subunit also makes two unusual interactions. First, it forms an interchain disulfide, connecting it to the phospholipase subunit. Second, it has an ion channel binding surface that resides roughly 30 Å away, and at the opposite end of the module, from the region homologous to the anti-protease loop.

The Kunitz module is one of the most extensively characterized structural motifs. Thus, the existence of a novel mode of interaction is both remarkable and unexpected. It demonstrates the ability of these modules to function in diverse contexts. Interestingly, the ion channel binding motif involves the only exposed loop (other than the anti-protease loop) connecting two strands in the Kunitz fold. This may be no coincidence; as has been found with immunoglobulins, loop regions often possess the advantages, such as an exposed surface area and a relative lack of sequence constraint, necessary to accommodate a functional interface.

Comparison of the ion channel binding motif that we have identified here with neuroactive peptides, suggests that the mode of binding of this class of toxins to K^+ channels may be analogous to that of endogenous neuropeptides. This implies that these particular neuropeptides may regulate their target channels by direct binding rather than indirectly through second messenger systems, as current thinking would impute.

Analysis of the phospholipase subunit reveals the functional mechanisms of neurotoxic action and may explain the active-site occlusion previously observed in the structures of several venom phospholipases. These mechanisms also make β-bungarotoxin a particularly attractive candidate for therapeutic adaptation. Not only does it lack hemolytic activity, but the targeting activity is segregated to a separate subunit. In addition, the calcium-dependent nature of the phospholipase confines lipolytic hydrolysis to the extracellular surface, thus safe-guarding intracellular machinery and reducing toxicity and the rate of metabolic inactivation. Most pathological cells should be sensitive to lipolytic degradation. Moreover, by recoupling the phospholipase to a viral receptor moiety, such phospholipase therapy may also work on enveloped virions. The biochemical inertness which makes virions resistant to conventional directed toxins should make them particularly sensitive to phospholipase degradation.

Materials and methods

Protein purification and crystallization

β_2-bungarotoxin was purified from the venom of *Bungarus multicinctus* (Miami Serpentarium) as previously described [6], except that an additional Mono-S (Pharmacia, Piscataway, NJ) chromatographic step at pH 8.8 was included. Crystals (space group $P4_322$; cell dimensions a=52.6 Å, c=177.5 Å; one molecule per asymmetric unit) were grown from hanging droplets composed of 7 μl of 10 mg ml^{-1} protein, 0.5 mM EDTA, 0.01% NaN_3, 1.4 M NaCl, equilibrated over 1.0 ml reservoirs of 3.3 M NaCl, 50 mM Tris-HCl, pH 8.5 at 20°C.

Data collection and molecular replacement

Data were collected on a Xuong–Hamlin area detector using CuKα radiation from a Rigaku rotating anode. Molecular replacement phasing as implemented in X-PLOR [61] was attempted using a model of bovine phospholipase A_2 [62] that included backbone atoms and conserved amino acid side chains. Using data with Bragg spacings between 10–4 Å, Patterson correlation refinement [63] resulted in a dominant rotation peak (0.079 correlation, 20% higher than the next highest peak) which produced a clear translation solution

(0.286 correlation in $P4_322$ against 0.190 in $P4_122$). After rigid-body refinement (correlation 0.329), the contribution of each amino acid to the correlation was checked by successive deletions, and the search model pruned accordingly. This improved the correlation to 0.419. Visual inspection of electron-density maps produced with these phospholipase model phases failed to give an indication of the orientation of the Kunitz subunit. Molecular replacement searches with numerous BPTI models also failed.

MIR, model building and refinement

A 20 mM $BaCl_2$ derivative was prepared by co-crystallization. Other derivatives (5 mM, 24 h equilibration) were screened using crystals stabilized in 4.75 M NaCl, 50 mM Tris-HCl, pH 8.5 (Table 1). Derivative atom positions were determined from difference Fourier maps by using the phospholipase model phases. Native and derivatives with different stabilization conditions were kept separate through heavy-atom refinement and phase calculations (REFINE and PHASE [64]), until protein ABCD coefficients could be combined [65]. Each derivative contained a single site. Anomalous differences were included in all heavy-atom calculations. A model for the phospholipase subunit was built into the MIR electron density. Phase combination between this model and the experimental MIR allowed the entire β_2-bungarotoxin model to be built. Subsequent refinement (X-PLOR) reduced the R value to 0.193 (5–2.45 Å, all data $>2\sigma$, with 10% of the data removed for free R value calculation [66]) with tightly restrained individual isotropic B values, and rmsds for bond lengths and angles of 0.011 Å and 1.6° respectively. The present model contains 1523 non-hydrogen atoms including 81 waters and 2 Na^+ ions. Both Na^+ ions are bound to the phospholipase. One is coordinated by a side-chain oxygen atom of Asp39 and the carbonyl oxygen atom of Glu105 (modeling it as a water produces unrealistically low temperature factors). The other is modeled into the calcium-binding loop (the crystallization medium contained EDTA which chelated all free calcium, and NaCl in excess of 3 M). The free R value [66] is 0.281.

β_2-bungarotoxin protein sequencing

Kunitz subunit: It was clear from the initial electron-density maps that the published sequence of the Kunitz subunit of β_2-bungarotoxin [6] was incorrect. We resequenced the Kunitz subunit using material purified for crystallization. The disulfide bonds of β_2-bungarotoxin were reduced and alkylated with iodoacetamide. After purification on reverse-phase HPLC, the reduced and alkylated Kunitz subunit was proteolyzed with endoproteinase Lys-C. Resulting peptides were separated by reverse phase HPLC and sequenced on an Applied Biosystems 470A sequencer (Applied Biosystems, Foster City, CA). The revised sequence is shown in Figure 3.

Phospholipase subunit: The five reported β-bungarotoxin phospholipase sequences, three from protein sequencing [7] and two from cDNA nucleotide sequencing [67,68], show greater than 90% identity. We examined the experimental electron density at each phospholipase amino acid where isoform differences had been reported, and on this basis, made five substitutions to the reported β_2-bungarotoxin sequence [7]: S66Q, Q67S, G87A, Q103N, D105E. All of these substitutions conform to the reported nucleotide sequences (also, see note added in proof).

Calculation of solvent accessibility

The solvent-accessible surface area occluded by the subunit interface was calculated with the program GRASP [56]. For individual amino acids, the fractional solvent accessibility was calculated as the ratio of the solvent-accessible surface area for atoms of an amino acid residue X in the protein to that area obtained after reducing the structure to a Gly-X-Gly tripeptide [69].

Protease-binding loop identification for Kunitz protease inhibitors

Residues likely to comprise the protease-binding loop for Kunitz protease inhibitors were chosen based on criteria similar to those used to identify the ion channel binding region: solvent accessibility (>15%), conservation of amino acid identity within the protease inhibitors and not in β_2-bungarotoxin, and preservation of main-chain orientation. Unfortunately, the coordinates of only two Kunitz protease inhibitors are available, BPTI and the protease inhibitor domain of the β-amyloid protein precursor [70], whereas the ion channel binding analysis used four structures. To increase the number of protease

Table 1. Structure determination.

Parameter	Native 1	Native 2	$BaCl_2$	*p*-CMBS#	K_2PtBr_6
Crystal stabilization					
NaCl (M)	3.5	4.75	3.5	4.75	4.75
Data collection statistics					
Resolution (Å)	10–2.45	10–3.3	7–2.9	10–3.3	10–6.0
Observations	30515	17126	25777	17856	3400
Unique	9372	3758	5125	3738	551
with Bijvoets	–	–	4760	3528	538
Completeness (%)	96.4	93.1	91.7	92.7	92.6
with Bijvoets	–	–	85.2	87.5	90.4
R_{sym}* (%)	6.9	7.2	6.9	7.6	4.9
Phasing statistics					
Mean isomorphous difference†			0.175	0.256	0.132
Cullis R factor‡			0.550	0.571	0.577
Phasing power§: isomorphous			1.9	1.8	2.1
anomalous			0.8	0.6	0.4

*$R_{sym}=\Sigma|I_{obs}-I_{avg}|/\Sigma I_{avg}$. †The mean isomorphous difference is $\Sigma|F_{PH}-F_P|/\Sigma F_P$, where F_{PH} and F_P are are the derivative and native structure-factor amplitudes, respectively. ‡The Cullis R factor is $\Sigma|F_H(obs)-F_H(calc)|/\Sigma F_H(obs)$, where F_H is the heavy-atom structure-factor amplitude. §Phasing power is the mean amplitude of the heavy-atom structure factors, F_H, divided by E, the rms lack of closure error. #*para*-chloromercuribenzene sulphate.

inhibitors, we included cow colostrum trypsin inhibitor (CCTI) [71], and snail inhibitor K (SIK) [72], which were used in the original sequence comparison with β-bungarotoxin by Kondo *et al.* [6]. Three amino acids are identified by these criteria, Gly12, Pro13 and Ala16 (BPTI numbering). A review of the sequences of functional Kunitz protease inhibitors demonstrates that these three residues are highly conserved and that the substitution of virtually any other two Kunitz module sequences for CCTI or SIK would also identify this region. For the intervening residues, which comprise the anti-protease loop, residue 15 (cysteine) is conserved in the Kunitz toxins, and residue 16 is not absolutely conserved (lysine or arginine) (BPTI numbering). Thus, while the analysis correctly identifies the general region of interaction, it is by no means comprehensive and other amino acids may contribute to the binding interaction and not be detected.

Sequence searches

The Swiss Protein data bank was searched with the motif, $KXCX_7CX_{12}CRX_2C\Phi$, where Φ is a hydrophobic residue. All of the matches had previously been identified as toxin members of the Kunitz superfamily, except for toxin E from *Dendroaspis polylepis polylepis*. Toxin E was initially found to be toxic [73], but was later also found to inhibit trypsin, and the original toxicity was attributed to a contaminant [74]. Experimental data remain inconclusive. A review of the previously published sequences of dendrotoxins and non-toxic venom inhibitor homologs [42,43], the Ca^{2+} channel blocker calcicludine [41], as well as the redetermined β-bungarotoxin sequences (Fig. 3), confirms the specificity of the motif.

Analysis of phospholipase surface

The physical and chemical properties of surfaces of 14 phospholipase crystal structures were analyzed with GRASP [56]. These include toxins (β_2-bungarotoxin, notexin [33]), phospholipases without substrate (Protein Data Bank accession codes 1BP2, 1BPQ, 1P2P, 1POA, 1POD, 1PPA, 1PP2, 1PSH) and substrate complexes (1POB, 1POC, 1POE, 5P2P). All phospholipases, except for bee phospholipase (see below), were oriented to a common frame by superimposition onto β_2-bungarotoxin. Superpositions used the main-chain atoms of the three invariant helices that define the core. The rmsds ranged between 0.4 Å and 0.6 Å for the superimposed helices. The collection of substrate complexes aligned in this manner, showed similar substrate orientations. The solvent-accessible surface (as defined by a 1.4 Å probe) of each phospholipase, 7.5 Å from the hydrophobic acyl chains of this collection of superimposed substrates, was analyzed with respect to the chemical character of the underlying atoms. Side-chain atoms in Asp, Glu, Lys and Arg residues were considered charged, carbon atoms in Val, Ile, Leu, Met, Trp and Tyr residues, hydrophobic, and all other atoms, including the backbone, polar. Quantitative measurements were made by calculating the surface area covering atoms of each chemical characteristic. (Because of its structural divergence, bee phospholipase could not be oriented by its protein structure. The bee phospholipase–substrate complex [1POC] was oriented by superimposing its substrate onto the substrate of the *Naja naja atra* complex [1POB]. The rmsd of superposition was 0.89 Å for the 24 atoms that remained within 2 Å of each other after least-squares alignment. The 7.5 Å radius surface analysis of 1POC was based solely on its own substrate. Despite the modified procedure, the hydrophobicity and surface area of the bee phospholipase–substrate complex were indistinguishable from other non-toxic phospholipases.)

Atomic coordinates for the β_2-bungarotoxin structure have been deposited with the Brookhaven Protein Data Bank.

Note added in proof

In a recent characterization of the β-bungarotoxin isoforms [77], additional isoform diversity is described and confirms four of the five phospholipase sequence changes proposed here.

Acknowledgements: We thank Mary Ann Gawinowicz for protein sequencing of the Kunitz subunit of β_2-bungarotoxin, Leonard A Smith for communication of results before publication and Lawrence Shapiro for a thorough reading of the manuscript. Research was supported by NIH grants, GM22324 and NS25867 (both to PBS), an NSF predoctoral fellowship (to PDK), and by the Howard Hughes Medical Institute.

References

1. Karalliedde, L. (1995). Animal toxins. *Br. J. Anaesth.* **74**, 319–327.
2. Jerusalinsky, D. & Harvey, A.L. (1994). Toxins from mamba venoms: small proteins with selectivities for different subtypes of muscarinic acetylcholine receptors. *Trends Pharmacol. Sci.* **15**, 424–430.
3. Chang, C.C. & Lee, C.Y. (1963). Isolation of neurotoxins from the venom of *Bungarus multicinctus* and their modes of neuromuscular blocking action. *Arch. Int. Pharmocodyn. Ter.* **144**, 241–257.
4. Abe, T., Stefano, A. & Miledi, R. (1977). Isolation and characterization of presynaptically acting neurotoxins from the venom of *Bungarus* snakes. *Eur. J. Biochem.* **80**, 1–12.
5. Wolf, K.M., Ciarleglio, A. & Chiappinelli, V.A. (1988). κ-bungarotoxin: binding of a neuronal nicotinic receptor antagonist to chick optic lobe and skeletal muscle. *Brain Res.* **439**, 249–258.
6. Kondo, K., Toda, H., Narita, K. & Lee, C.-Y. (1982). Amino acid sequence of β_2-bungarotoxin from *Bungarus multicinctus* venom. The amino acid substitutions in the B chains. *J. Biochem.* **91**, 1519–1530.
7. Kondo, K., Toda, H., Narita, K. & Lee, C.-Y. (1982). Amino acid sequences of three β-bungarotoxins (β_3-, β_4-, and β_5-bungarotoxin) from *Bungarus multicinctus* venom. Amino acid substitutions in the A chains. *J. Biochem.* **91**, 1531–1548.
8. Scott, D.L., White, S.P., Otwinowski, Z., Yuan, W., Gelb, M.H. & Sigler, P.B. (1990). Interfacial catalysis: the mechanism of phospholipase A_2. *Science* **250**, 1541–1546.
9. Dennis, E.A. (1994). Diversity of group types, regulation, and function of phospholipase A_2. *J. Biol. Chem.* **269**, 13057–13060.
10. Rugolo, M., Dolly, J.O. & Nicholls, D.G. (1986). The mechanism of action of β-bungarotoxin at the presynaptic plasma membrane. *Biochem. J.* **233**, 519–523.
11. Laskowski, M. & Kato, I. (1980). Protein inhibitors of proteinases. *Annu. Rev. Biochem.* **49**, 593–626.
12. Bode, W. & Huber, R. (1992). Natural protein proteinase inhibitors and their interaction with proteinases. *Eur. J. Biochem.* **204**, 433–451.
13. Rehm, H. & Betz, H. (1984). Solubilization and characterization of the beta-bungarotoxin-binding protein of chick brain membranes. *J. Biol. Chem.* **259**, 6865–6869.
14. Petersen, M., Penner, R., Pierau, F.-K. & Deyer, F. (1986). Beta-bungarotoxin inhibits a non-inactivating potassium current in guinea pig dorsal root ganglion neurons. *Neurosci. Lett.* **68**, 141–145.
15. Rehm, H. & Tempel, B.L. (1991). Voltage-gated K^+ channels of the mammalian brain. *FASEB J.* **15**, 164–170.
16. Chang, C.C. (1985). Neurotoxins with phospholipase A_2 activity in snake venoms. *Proc. Natl. Sci. Counc. B. ROC* **9**, 126–142.
17. Radvanyi, F., Saliou, B., Bon, C. & Strong, P.N. (1987). The interaction between the presynaptic phospholipase neurotoxins β-bungarotoxin and crotoxin and mixed detergent=phosphatidylcholine micelles. *J. Biol. Chem.* **262**, 8966–8974.
18. Delot, E. & Bon, C. (1993). Model for the interaction of crotoxin, a phospholipase A_2 neurotoxin, with presynaptic membranes. *Biochemistry* **32**, 10708–10713.
19. Lambeau, G., Schmid-Alliana, A., Lazdunski, M. & Barhanin, J. (1990). Identification and purification of a very high affinity binding protein for toxic phospholipases A_2 in skeletal muscle. *J. Biol. Chem.* **265**, 9526–9532.
20. Harris, J.B., Karlsson, E. & Thesleff, S. (1973). Effects of an isolated toxin from Australian Tiger snake (*Notechis scutatus scutatus*) venom at the mammalian neuromuscular junction. *Br. J. Pharmacol.* **47**, 141–146
21. Skarzynski, T. (1992). Crystal structure of α-dendrotoxin from the green mamba venom and its comparison with the structure of bovine pancreatic trypsin inhibitor. *J. Mol. Biol.* **224**, 671–683.
22. Lancelin, J.-M., Foray, M.-F., Poncin, M., Hollecker, M. & Marion, D. (1994). Proteinase inhibitor homologues as potassium channel blockers. *Nat. Struct. Biol.* **1**, 246–250.

23. Berndt, K.D., Güntert, P. & Wüthrich, K. (1993). Nuclear magnetic resonance solution structure of dendrotoxin K from the venom of *Dendroaspis polylepis polylepis*. *J. Mol. Biol.* **234**, 735–750.
24. Black, A.R., Donegan, C.M., Denny, B.J. & Dolly, J.O. (1988). Solubilization and physical characterization of acceptors for dendrotoxin and β-bungarotoxin from synaptic membranes of rat brain. *Biochemistry* **27**, 6814–6820.
25. Benishin, C.G. (1990). Potassium channel blockade by the B subunit of β-bungarotoxin. *Mol. Pharmacol.* **38**, 164–169.
26. Chang, C.H., Chen, T.F. & Lee, C.Y. (1973). Studies on the presynaptic effect of β-bungarotoxin on neuromuscular transmission. *J. Pharmacol. Exp. Ther.* **184**, 339–345.
27. Smith, L.A., Lafaye, P.J., LaPenotiere, H.F., Spain, T. & Dolly, J.O. (1993). Cloning and functional expression of dendrotoxin K from Black Mamba, a K^+ channel blocker. *Biochemistry* **32**, 5692–5697.
28. Harvey, A.L., Rowan, E.G., Vatapour, H., Fatehi, M., Castaneda, O. & Karlsson, E. (1994). Potassium channel toxins and transmitter release. *Ann. N.Y. Acad. Sci.* **710**, 1–10.
29. FitzGerald, D. & Pastan, I. (1989). Targeted toxin therapy for the treatment of cancer. *J. Nat. Cancer Inst.* **81**, 1455–1463.
30. Press, O.W. (1991). Immunotoxins. *Biotherapy* **3**, 65–76.
31. Ho, C.L., Ko, J.L. & Lee, C.Y. (1986). Differences in pharmacological actions between beta-bungarotoxin and other neurotoxic phospholipases A_2 purified from snake venoms. *Proc. Natl. Sci. Counc. B. ROC* **10**, 196–202.
32. Politi, L.E. & Adler, R. (1986). Generation of enriched populations of cultured photoreceptor cells. *Invest. Ophthalmol. Vis. Sci.* **27**, 656–665.
33. Westerlund, B., Nordlund, P., Uhlin, U., Eaker, D. & Eklund, H. (1992). The three-dimensional structure of notexin, a presynaptic neurotoxic phospholipase A_2 at 2.0 Å resolution. *Fed. Eur. Biochem. Soc.* **301**, 159–164.
34. Huber, R., Kukla, D., Ruehlmann, A., Epp, O. & Formanek, H. (1970). Basic trypsin inhibitor of bovine pancreas. 1. Structure-analysis and conformation of polypeptide-chain. *Naturwissenschaften* **57**, 389–392.
35. Deisenhofer, J. & Stiegemann, W. (1975). Crystallographic refinement of structure of bovine pancreatic trypsin inhibitor at 1.5 Å resolution. *Acta Cryst. B* **31**, 238–250.
36. Schmidt, T., Stumm-Zollinger, E., Chen, P.-S., Böhlen, P. & Stone, S.R. (1989). A male accessory gland peptide with protease inhibitory activity in *Drosophila funebris*. *J. Biol. Chem.* **264**, 9745–9749.
37. Housset, D., Kim, K.S., Fuchs, J., Woodward, C. & Wlodawer, A. (1991). Crystal structure of a Y35G mutant of bovine pancreatic trypsin inhibitor. *J. Mol. Biol.* **220**, 757–770.
38. Kuipers, O.P., *et al.*, & de Haas, G.H. (1989). Enhanced activity and altered specificity of phospholipase A_2 by deletion of a surface loop. *Science* **244**, 82–85.
39. Smith, W.C. & Harland, R.M. (1992). Expression cloning of noggin, a new dorsalizing factor localized to the Spemann organizer in *Xenopus* embryos. *Cell* **70**, 829–840.
40. McDonald, N.Q. & Kwong, P.D. (1993). Does noggin head a new class of Kunitz domain? *Trends Biochem. Sci.* **18**, 208–209.
41. Schweitz, H., Heurteaux, C., Bois, P., Moinier, D., Romey, G. & Lazdunski, M. (1994). Calcicludine, a venom peptide of the Kunitz-type protease inhibitor family, is a potent blocker of high-threshold Ca^{2+} channels with a high affinity for L-type channels in cerebellar granule neurons. *Proc. Natl. Acad. Sci. USA* **91**, 878–882.
42. Joubert, F.J. & Taljaard, N. (1980). The amino acid sequences of two proteinase inhibitor homologues from *Dendroaspis angusticeps* venom. *Hoppe-Seyler's Z. Physiol. Chem.* **361**, 661–674.
43. Harvey, A.L., Anderson, A.J. & Karlsson, E. (1984). Facilitation of transmitter release by neurotoxins from snake venoms. *J. Physiol.* **79**, 222–227.
44. Dufton, M.J. (1985). Proteinase inhibitors and dendrotoxins. Sequence classifications, structural prediction and structure/activity. *Eur. J. Biochem.* **153**, 647–654.
45. Hurst, R.S., Busch, A.E., Kavanaugh, M.P., Osborne, P.B., North, R.A. & Adelman, J.P. (1991). Identification of amino acid residues involved in dendrotoxin block of rat voltage-dependent potassium channels. *Mol. Pharmacol.* **40**, 572–576.
46. Stocker, M., *et al.*, & Ruppersberg, J.P. (1991). Swapping of functional domains in voltage-gated K^+ channels. *Proc. R. Soc. Lond.* **245**, 101–107.
47. Bidard, J.-N., Mourre, C. & Lazdunski, M. (1987). Two potent central convulsant peptides, a bee venom toxin, the MCD peptide, and a snake venom toxin, dendrotoxin I, known to block K^+ channels, have interacting receptor sites. *Biochem. Biophys. Res. Commun.* **143**, 383–389.
48. Cherubini, E., Ari, Y.B., Gho, M., Bidard, J.N. & Lazdunski, M. (1987). Long-term potentiation of synaptic transmission in the hippocampus induced by a bee venom peptide. *Nature* **328**, 70–73.
49. Kumar, N.V., Wemmer, D.E. & Kallenbach, N.R. (1988). Structure of P401 (mast cell degranulating peptide) in solution. *Biophys. Chem.* **31**, 113–119.
50. Contrell, G.A., Green, K.A. & Davies, N.W. (1990). The neuropeptide Phe-Met-Arg-Phe-NH_2 (FMRFamide) can activate a ligand-gated ion channel in *Helix* neurones. *Pflügers Arch.* **416**, 612–614.
51. Hökfelt, T. (1991). Neuropeptides in perspective: the last ten years. *Neuron* **7**, 867–879.
52. Fuxe, K., Li, X.M., Bjelke, B., Hedlund P.B., Biagini, G. & Agnati L.F. (1994). Possible mechanisms for the powerful actions of neuropeptides. *Ann. N.Y. Acad. Sci.* **739**, 42–59.
53. Hugues, M., Romey, G., Duval, D., Vincent, J.P. & Lazdunski, M. (1982). Apamin as a selective blocker of the calcium dependent potassium channel in neuroblastoma cells: voltage clamp and biochemical characterization of the toxin receptor. *Proc. Natl. Acad. Sci. USA* **79**, 1308–1312.
54. Fosset, M., Schmid-Antomarchi, H., Hugues, M., Romey, G. & Lazdunski, M. (1984). The presence in pig brain of an endogenous equivalent of apamin, the bee venom peptide that specifically blocks Ca^{2+}-dependent K^+ channels. *Proc. Natl. Acad. Sci. USA* **81**, 7228–7232.
55. Maraganore, J.M. & Heinrikson, R.L. (1986). The lysine-49 phospholipase A_2 from the venom of *Agkistondon piscivorus piscivorus*. Relation of structure and function to other phospholipases A_2. *J. Biol. Chem.* **261**, 4797–4804.
56. Nicholls, A., Sharp, K.A. & Honig, B. (1991). Protein folding and association: insights from the interfacial and thermodynamic properties of hydrocarbons. *Proteins* **11**, 281–296.
57. Ponder, J.W. & Richards, F.M. (1987). Tertiary templates for proteins: use of packing criteria in the enumeration of allowed sequences for different structural classes. *J. Mol. Biol.* **193**, 775–791.
58. Brunie, S., Bolin, J., Gewirth, D. & Sigler, P.B. (1985). The refined crystal structure of dimeric phospholipase A_2 at 2.5 Å. Access to a shielded catalytic center. *J. Biol. Chem.* **260**, 9742–9749.
59. Fremont, D.H., Anderson, D.H., Wilson, I.A., Dennis, E.A. & Xuong, N.H. (1993). Crystal structure of phospholipase A_2 from Indian cobra reveals a trimeric association. *Proc. Natl. Acad. Sci. USA* **90**, 342–346.
60. Hudson, T.H. & Grillo, F.G. (1991). Brefeldin-A enhancement of ricin A-chain immunotoxins and blockade of intact ricin, modeccin, and abrin. *J. Biol. Chem.* **266**, 18586–18592.
61. Brünger, A.T. (1992). *X-PLOR Manual, Version 3.1*. Yale University, New Haven, CT.
62. Dijkstra, B.W., Kalk, K.H., Hol, W.G.J. & Drenth, J. (1981). Structure of bovine pancreatic phospholipase A_2 at 1.7 Å resolution. *J. Mol. Biol.* **147**, 97–123.
63. Brünger, A.T. (1990). Extension of molecular replacement: a new search strategy based on Patterson correlation refinement. *Acta Cryst. B* **44**, 46–57.
64. Collaborative Computational Project, Number 4 (1994). The CCP4 suite: programs for protein crystallography. *Acta Cryst. D* **50**, 760–763.
65. Hendrickson, W.A. & Lattman, E.E. (1970). Representation of phase probability distributions for simplified combination of independent phase information. *Acta Cryst. B* **26**, 136–143.
66. Brünger, A.T. (1992). Free R value: a novel statistical quantity for assessing the accuracy of crystal structures. *Nature* **355**, 472–475.
67. Danse, J.-M., Toussaint, J.-L. & Kempf, J. (1990). Nucleotide sequence encoding β-bungarotoxin A_2-chain from the venom of *Bungarus multicinctus*. *Nucleic Acids Res.* **18**, 4609.
68. Danse, J.-M., Garnier, J.-M. & Kempf, J. (1990). cDNA deduced amino-acid sequence of a new phospholipase from *Bungarus multicinctus*. *Nucleic Acids Res.* **18**, 4610.
69. Sheriff, S., Hendrickson, W.A., Stenkamp, R.E., Sieker, L.C. & Jensen, L.H. (1985). Influence of solvent accessibility and intermolecular contacts on atomic mobilities in hemerythrins. *Proc. Natl. Acad. Sci. USA* **82**, 1104–1107.
70. Hynes, T.R., Randal, M., Kennedy, L.A., Eigenbrot, C. & Kossiakoff, A.A. (1990). X-ray crystal structure of the protease inhibitor domain of Alzheimer's amyloid β-protein precursor. *Biochemistry* **29**, 10018–10022.
71. Cechova, D. (1976). Trypsin inhibitor from cow colostrum. *Methods Enzymol.* **45**, 806–813.
72. Tschesche, H. & Dietl, T. (1975). The amino-acid sequence of isoinhibitor K from snails (*Helix pomatia*). A sequence determination by automated Edman degradation and mass-spectral identification of the phenylthiohydantoins. *Eur. J. Biochem.* **58**, 439–451.
73. Strydom, D.J. (1976). Snake venom toxins: purification and properties of low-molecular-weight polypeptides of *Dendroaspis polylepis polylepis* (Black Mamba) venom. *Eur. J. Biochem.* **69**, 169–176.
74. Joubert, F.J. & Strydom, D.J. (1978). Snake venoms: the amino-acid sequence of trypsin inhibitor E of *Dendroaspis polylepis polylepis* (Black Mamba) venom. *Eur. J. Biochem.* **87**, 191–198.
75. Evans, S.V. (1993). SETOR — hardware-lighted three-dimensional solid model representations of macromolecules. *J. Mol. Graphics* **11**, 134–138.
76. Kraulis, P.J. (1991). MOLSCRIPT: a program to produce both detailed and schematic plots of proteins. *J. Appl. Cryst.* **24**, 946–950.
77. Chu, C.-C., Li, S.-H. & Chen, Y.-H. (1995). Resolution of isotoxins in the β-bungarotoxin family. *J. Chromatogr. A* **694**, 492–497.

Received: **22 May 1995**; revisions requested: **23 Jun 1995**; revisions received: **18 Aug 1995**. Accepted: **23 Aug 1995**.